DNA Aptamer Raised Against AGEs Blocks the Progression of Experimental Diabetic Nephropathy

Yusuke Kaida,[1] Kei Fukami,[1] Takanori Matsui,[2] Yuichiro Higashimoto,[3] Yuri Nishino,[2] Nana Obara,[1] Yosuke Nakayama,[1] Ryotaro Ando,[1] Maki Toyonaga,[1] Seiji Ueda,[1] Masayoshi Takeuchi,[4] Hiroyoshi Inoue,[5] Seiya Okuda,[1] and Sho-ichi Yamagishi[2]

Advanced glycation end products (AGEs) and their receptor (RAGE) play a role in diabetic nephropathy. We screened DNA aptamer directed against AGEs (AGEs-aptamer) in vitro and examined its effects on renal injury in KKAy/Ta mice, an animal model of type 2 diabetes. Eight-week-old male KKAy/Ta or C57BL/6J mice received continuous intraperitoneal infusion of AGEs- or control-aptamer for 8 weeks. AGEs-aptamer was detected and its level was increased in the kidney for at least 7 days. The elimination half-lives of AGEs-aptamer in the kidney were about 7 days. Compared with those in C57BL/6J mice, glomerular AGEs levels were significantly increased in KKAy/Ta mice, which were blocked by AGEs-aptamer. Urinary albumin and 8-hydroxy-2′-deoxy-guanosine levels were increased, and glomerular hypertrophy and enhanced extracellular matrix accumulation were observed in KKAy/Ta mice, all of which were prevented by AGEs-aptamer. Moreover, AGEs-aptamer significantly reduced gene expression of *RAGE*, monocyte chemoattractant protein-1, connective tissue growth factor, and type IV collagen both in the kidney of KKAy/Ta mice and in AGE-exposed human cultured mesangial cells. Our present data suggest that continuous administration of AGEs-aptamer could protect against experimental diabetic nephropathy by blocking the AGEs-RAGE axis and may be a feasible and promising therapeutic strategy for the treatment of diabetic nephropathy. ***Diabetes* 62:3241–3250, 2013**

Diabetic nephropathy is a leading cause of end-stage renal disease, which accounts for disability and high mortality rate in patients with diabetes (1,2). The development of diabetic nephropathy is characterized by glomerular hypertrophy and inflammatory cell infiltration, followed by extracellular matrix (ECM) accumulation in mesangial area and an increased urinary albumin excretion (UAE) rate (3). Diabetic nephropathy ultimately progresses glomerular sclerosis associated with renal dysfunction (4). Large-scale clinical studies have shown that intensive glycemic and blood pressure control reduce the risk of diabetic

nephropathy (5). However, management of diabetic nephropathy is far from satisfactory because strict control of blood glucose or pressure is often difficult to maintain and may increase the risk of hypoglycemia or hypotension. Further, despite intensive management of classical cardiovascular risk factors using blood pressure–lowering and lipid-lowering agents, a substantial number of diabetic patients still have experienced end-stage renal disease. Therefore, development of novel therapeutic strategies that specifically target diabetic nephropathy is urgently needed.

Reducing sugars can react nonenzymatically with the amino groups of proteins to initiate a complex series of rearrangements and dehydrations and then to produce a class of irreversibly cross-linked moieties termed advanced glycation end products (AGEs) (6–8). The formation and accumulation of AGEs in various tissues have been shown to progress at an accelerated rate under hyperglycemic conditions (9–11). There is accumulating evidence that AGE and RAGE (receptor for AGEs) interaction stimulates oxidative stress generation and subsequently evokes inflammatory reactions, thereby causing progressive alteration in renal architecture and loss of renal function in diabetes (12–14). Indeed, inhibitors of AGE formation have been shown to attenuate the increase in albuminuria and prevent the development and progression of experimental diabetic nephropathy (15,16). Further, RAGE-overexpressing diabetic mice have shown progressive glomerulosclerosis with renal dysfunction, while diabetic homozygous RAGE-null mice failed to develop significantly increased mesangial matrix expansion or thickening of the glomerular basement membrane (14,17). These observations suggest that the inhibition of the AGE-RAGE axis could be a novel therapeutic target for diabetic nephropathy.

Aptamers are short, single-stranded DNA or RNA molecules that can bind with high affinity and specificity to a wide range of target proteins (18). Recently, numerous aptamers have been developed and used in the clinical fields as a tool for modulating various protein function (19–21). Pegaptanib, an RNA aptamer directed against vascular endothelial growth factor (VEGF)$_{165}$ isoform, has been shown to be effective in treating choroidal neovascularization in patients with age-related macular degeneration (19). In addition, ARC1779, a DNA-aptamer raised against the A1 domain of von Willebrand factor, has also been reported to inhibit its prothrombotic function in vivo, and phase II clinical trials of ARC1779 are currently underway for the treatment of thrombotic thrombocytopenic purpura and cerebral embolism after carotid endarterectomy (20,21).

Therefore, in this study we screened a high-affinity DNA aptamer directed against AGEs (AGEs-aptamer) using

a combinatorial chemistry in vitro and examined its effects on experimental diabetic nephropathy. For this, we chose KKAy/Ta mice because they are an animal model of obesity and type 2 diabetes associated with ECM accumulation, inflammatory cell infiltration, and sclerotic changes within the glomerular areas, whose characteristics closely resemble those in human diabetic nephropathy (22). Furthermore, we investigated the effects of AGEs-aptamer on mesangial cell damage in vitro.

RESEARCH DESIGN AND METHODS

Animals. Male 8-week-old KKAy/Ta (DM) and 8-week-old C57BL/6J (Ctr) mice were purchased from CLEA Japan (Tokyo, Japan). These mice were divided into two groups respectively and received continuous infusion of either AGEs-aptamer or control-aptamer (Ctr-aptamer) (0.136 μg/day i.p.) by an osmotic minipump (model 1004; ALZET, Cupertino, CA) (Ctr-aptamer–treated Ctr mice [Ctr-Ctr-aptamer], $n = 8$; AGEs-aptamer–treated Ctr mice [Ctr-AGEs-aptamer], $n = 9$; Ctr-aptamer–treated DM mice [DM-Ctr-aptamer], $n = 11$; and AGEs-aptamer–treated DM mice [DM-AGEs-aptamer], $n = 10$ group). Eight weeks after the continuous intraperitoneal infusion, blood pressure was measured by a tail-cuff sphygmomanometer using an automated system with a photoelectric sensor (BP-98A; Softron, Tokyo, Japan), and mice were transferred to metabolic cages for 24 h for urinalysis. Then, mice were killed and blood and kidney samples were obtained. All experimental procedures were conducted in accordance with the National Institutes Health Guide for Care and Use of Laboratory Animals and were approved by the ethics committee of Kurume University School of Medicine.

Measurement of clinical variables. Albuminuria was determined with a commercially available ELISA kit (Exocell, Philadelphia, PA). Blood was collected and centrifuged, and plasma and serum were obtained and stored at –40°C. Total cholesterol and transaminase levels were determined by commercially available kits (Wako, Osaka, Japan). Plasma creatinine levels were measured by an enzymatic method (SRL, Tokyo, Japan). Blood urea nitrogen levels were measured by an auto-analyzer (Nihondenshi, Tokyo, Japan). Plasma glucose was measured by a glucose oxidase method (Shionotest, Tokyo, Japan). HbA$_{1c}$ was determined by a latex coagulation method (TFB, Tokyo, Japan). Urinary 8-hydroxy-2′-deoxy-guanosine (8-OHdG) levels were measured with an ELISA system (Japan Institute for the Control of Aging, Shizuoka, Japan). Urinary N-acetyl-β-D-glucosaminidase was measured with a fractional colorimetric determination method (Shionogi Pharma, Osaka, Japan). Intra- and interassay coefficients of variation were 6.2 and 8.8%, respectively.

Preparation of AGEs–human serum albumin and AGEs-BSA. AGE-modified proteins were prepared as previously described (23).

Immobilizing AGEs–human serum albumin on agarose beads. AGEs–human serum albumin (AGEs-HSA) was covalently coupled to indoacetyl groups on SulfoLink Coupling Gel (Pierce, Rockford, IL) as previously described (24).

Screening and modification of AGEs-aptamer (Systematic Evolution of Ligands by EXponential enrichment). Preparation and selection of DNA aptamers were performed as previously described (24). Sequences of AGEs- and Ctr-DNA aptamers are follows: AGEs-aptamer, 5′-CCGAAACCA-GACCACCCCACCAAGGCCACTCGGTCGAACCGCCAACACTCACCCCA-3′; Ctr-aptamer, 5′-GTTATCTGTCATAGGAACAGTCAGACTCAGCGTCGCAGT TCAGGGCACTTTAGCAC-3′. DNA aptamers are susceptible to degradation by nucleases. This will limit their applications for real samples, such as blood and tissues. To solve this issue, we modified aptamers with phosphorothioate as previously described (25).

Binding affinity of AGEs-aptamer to AGEs-HSA or AGEs-HSA to RAGE. The binding affinity of the selected AGEs-aptamer to AGEs-HSA or AGEs-HSA to extracellular AGEs-binding V-domain of RAGE (vRAGE) was measured using sensitive 27-MHz quartz crystal microbalance (QCM) (Affinix Q; Initium, Tokyo, Japan) according to the method of Okahata et al. (26). In brief, AGEs-HSA or vRAGE was immobilized on an avidin-bound QCM surface. After adding Ctr-aptamer or AGEs-aptamer to a reaction vessel in the presence or absence of 70 ng/mL AGEs-HSA, the time course of the frequency decrease of bound AGEs-HSA or bound vRAGE on the QCM was monitored. The binding affinity of AGEs-aptamer to AGEs-HSA or AGEs-HSA to vRAGE was calculated from curve fitting to the QCM frequency decrease. Human vRAGE (residues 23–121) was prepared as previously described (27,28). SDS-PAGE analysis of purified vRAGE proteins revealed a single band, which showed positive reactivity with polyclonal antibody raised against RAGE (data not shown).

Distribution and kinetics of [γ-^{32}P]ATP-labeled AGEs-aptamer. Aptamer was radioactively labeled by a 5′-end-labeling technique using T4 polynucleotide kinase (T4 PNK; Promega, Madison, WI) and [γ-^{32}P]ATP (PerkinElmer Japan, Kanagawa, Japan) according to the manufacturer's protocol. Male

8-week-old Ctr mice received continuous infusion of [γ-^{32}P]ATP-labeled AGEs-aptamer (0.136 μg/day i.p.) by an osmotic minipump, and were killed at 0 h, 1 h, 6 h, 1 day, 2 days, and 7 days after the infusion. At 0, 3, 7, and 14 days after stopping the infusion, mice were killed and blood and organs obtained. The radioactivity of AGEs-aptamer was measured by Cherenkov counting using an LS-6500 scintillation counter (Beckman Coulter, San Francisco, CA).

Turnover rate of aptamer-bound AGEs by macrophages. Human THP-1 monocytic leukemia cells were differentiated to macrophages as previously described (29). AGEs-BSA (100 μg/mL) was added to the culture medium in the presence or absence of 2 μmol/L AGEs-aptamer where differentiated THP-1 macrophages were grown or ungrown. After 4 h, the supernatant was collected, concentrated with Amicon Urtra centrifugal filter (Millipore, Billerica, MA), separated by SDS-PAGE, and transferred to polyvinylidene fluoride membrane as previously described (30). Membranes were probed with rabbit polyclonal antibodies raised against AGEs, and then immune complexes were visualized with an enhanced chemiluminescence detection system (Amersham Bioscience, Buckinghamshire, U.K.).

Morphological analysis. Three-micrometer paraffin sections were stained with periodic acid Schiff and Masson trichrome for light microscopic analysis as previously described (31).

Measurement of serum AGEs. Measurement of serum AGE levels was performed with a competitive ELISA as previously described (32).

Immunostaining. Specimens of kidney cortex were fixed with 4% paraformaldehyde, embedded in paraffin, sectioned at 4-μm intervals, and mounted on glass slides. The sections were incubated in 0.3% hydrogen peroxide methanol for 30 min and incubated overnight at 4°C with rabbit polyclonal antibodies raised against AGEs and synaptopodin (PROGEN Biotechnik, Heidelberg, Germany) as previously described (32). Immunoreactivity in 10 different fields (×600) in each sample was measured by image-analysis software (version 6.57; Optimas, Media Cybernetics, Silver Spring, MD).

Cells. Human mesangial cells were maintained in basal medium supplemented with 5% FBS according to the supplier's instructions (Clonetics, San Diego, CA). AGE treatment was carried out in a medium containing 0.5% FBS. Mesangial cells less than six passages were used for the experiments. Mesangial cells were treated with 100 μg/mL AGEs-BSA or nonglycated BSA for 4 and 24 h in the presence or absence of 0.2 or 2 μmol/L AGEs-aptamer.

Real-time RT-PCR. Total RNA (3–6 μg) extracted from each kidney cortex was used to synthesize cDNA with the Superscript First Strand synthesis system for RT-PCR (Invitrogen, Carlsbad, CA). Quantitative real-time RT-PCR was performed using Assay-on-Demand and TaqMan 5 fluorogenic nuclease chemistry (Applied Biosystems, Foster city, CA) according to the supplier's recommendation. Identifications of primers and probe for mouse monocyte chemoattractant protein-1 (MCP-1), tumor necrosis factor-α (TNF-α), connective tissue growth factor (CTGF), type IV collagen, VEGF, AGE-receptor 3 (AGE-R3), and RAGE genes were Mm00441242_ml, Mn00443258_m1, Mm01192933_g1, Mm01210125_m1, Mm01281449_m1, PN4331348, and Mm00545815_m1, respectively (Applied Biosystems). TaqMan Ribosomal RNA Control Reagents (18S) was used as an endogenous control (Applied Biosystems). Total RNAs were extracted from cultured human mesangial cells and THP-1 cells with an RNA queous-4 PCR kit (Ambion, Austin, TX), and quantitative real-time RT-PCR was performed. Identifications of primers and probe for human MCP-1, TNF-α, CTGF, RAGE, and glyceraldehyde-3-phosphate dehydrogenase (GAPDH) genes were Hs00234140_m1, Hs00170014_m1, Hs00174128_m1, Hs00153957_m1, and Hs99999905_m1, respectively (Applied Biosystems).

Measurement of reactive oxygen species generation. The intracellular formation of reactive oxygen species (ROS) was detected using the fluorescent probe CM-H$_2$DCFDA (Molecular Probes, Eugene, OR) as previously described (33).

Statistical analysis. All data are presented as means ± SEM. ANOVA followed by the Turkey or Games-Howell post hoc test was performed for all studied parameters for statistical comparisons; $P < 0.05$ was considered significant. All statistical analyses were performed with the SPSS 19 system.

RESULTS

Isolation and characterization of DNA aptamers directed against AGE-modified proteins. DNA aptamers specific for AGEs-HSA were isolated by an in vitro selection process, Systematic Evolution of Ligands by EXponential enrichment, from a pool of ~10^{15} different nucleic acid sequences as previously described (24). In this study, 35 clones were sequenced from the pool of selected single-stranded DNAs to obtain 15 unique sequences, indicating that some of the sequences among

the 35 clones were identified and that multiple selection of the same clone occurred. Structural analysis revealed that all of the aptamers had a bulge-loop structure with cytosine-rich sequences. We have previously shown that although all the clones significantly inhibited the AGEs-induced decrease in DNA synthesis in cultured pericytes, a counterpart of mesangial cells in the kidney, clone 1, had the strongest effect (24). So, we modified clone 1 with phosphorothioate for generating nuclease-resistant aptamer and used it for the following experiments. The structure of phosphorothioate AGEs-aptamer used here is shown in Fig. 1A.

Binding affinity of phosphorothioate AGEs-aptamer to AGEs-HSA or AGEs-HSA to vRAGE. We first examined the binding affinity of phosphorothioate AGEs-aptamer to AGEs-HSA in vitro. For this, AGEs-HSA was immobilized on an avidin-bound QCM surface, and then Ctr- or AGEs-aptamer was added to a reaction vessel. AGEs-aptamer bound to AGEs-HSA with a dissociation constant of 1.38×10^{-6} mol/L, whereas Ctr-aptamer did not bind to AGEs-HSA at all (Fig. 1B). Further, as shown in Fig. 1C, the binding of AGEs-HSA to vRAGE was dose-dependently inhibited by the cotreatment with AGEs-aptamer.

Turnover rate of aptamer-bound AGEs-BSA. Compared with unbound AGEs-BSA, turnover rate of aptamer-bound AGEs by differentiated THP-1 macrophages was more increased (Fig. 1D). On the contrary, under the conditions without THP-1 cells, presence of AGEs-aptamer did not affect the turnover rate of AGEs-BSA (Fig. 1E).

Distribution and kinetics of infused AGEs-aptamer. To examine the kinetics of injected AGEs-aptamer, we labeled the aptamer with $[\gamma\text{-}^{32}\text{P}]\text{ATP}$ and infused it into the peritoneal cavity of 8-week-old Ctr mice by an osmotic pump. As shown in Fig. 2A, when AGEs-aptamer was continuously administrated up to 7 days, it was distributed mainly in the kidney, aorta, and muscle. The levels of AGEs-aptamer were increased in the kidney, liver, and blood of 8-week old Ctr mice for at least 7 days after continuous 0.136 µg/day i.p. infusion (Fig. 2B). After the injection was stopped, AGEs-aptamer levels were gradually decreased. But the aptamer was still detected in the kidney, liver, and blood at day 14 after the removal of an osmotic pump (Fig. 2B). The elimination half-lives of AGEs-aptamer in the kidney were about 7 days.

Characteristics of animals. Clinical characteristics of each group are shown in Table 1. Compared with Ctr-Ctr-aptamer mice, body weight, plasma glucose, HbA_{1c}, and total cholesterol levels were significantly increased in DM-Ctr-aptamer mice ($P < 0.05$). Treatment with AGEs-aptamer did not affect these parameters in mice. Plasma levels of blood urea nitrogen and creatinine tended to be higher and kidney-to-body weight ratio was significantly increased in DM-Ctr-aptamer mice, which were ameliorated by the treatment of AGEs-aptamer ($P < 0.05$). There were no significant differences of clinical variables between Ctr-Ctr-aptamer and Ctr-AGEs-aptamer mice.

Effect of AGEs-aptamer on serum and renal levels of AGEs in mice. We investigated whether treatment with AGEs-aptamer could reduce serum and renal levels of
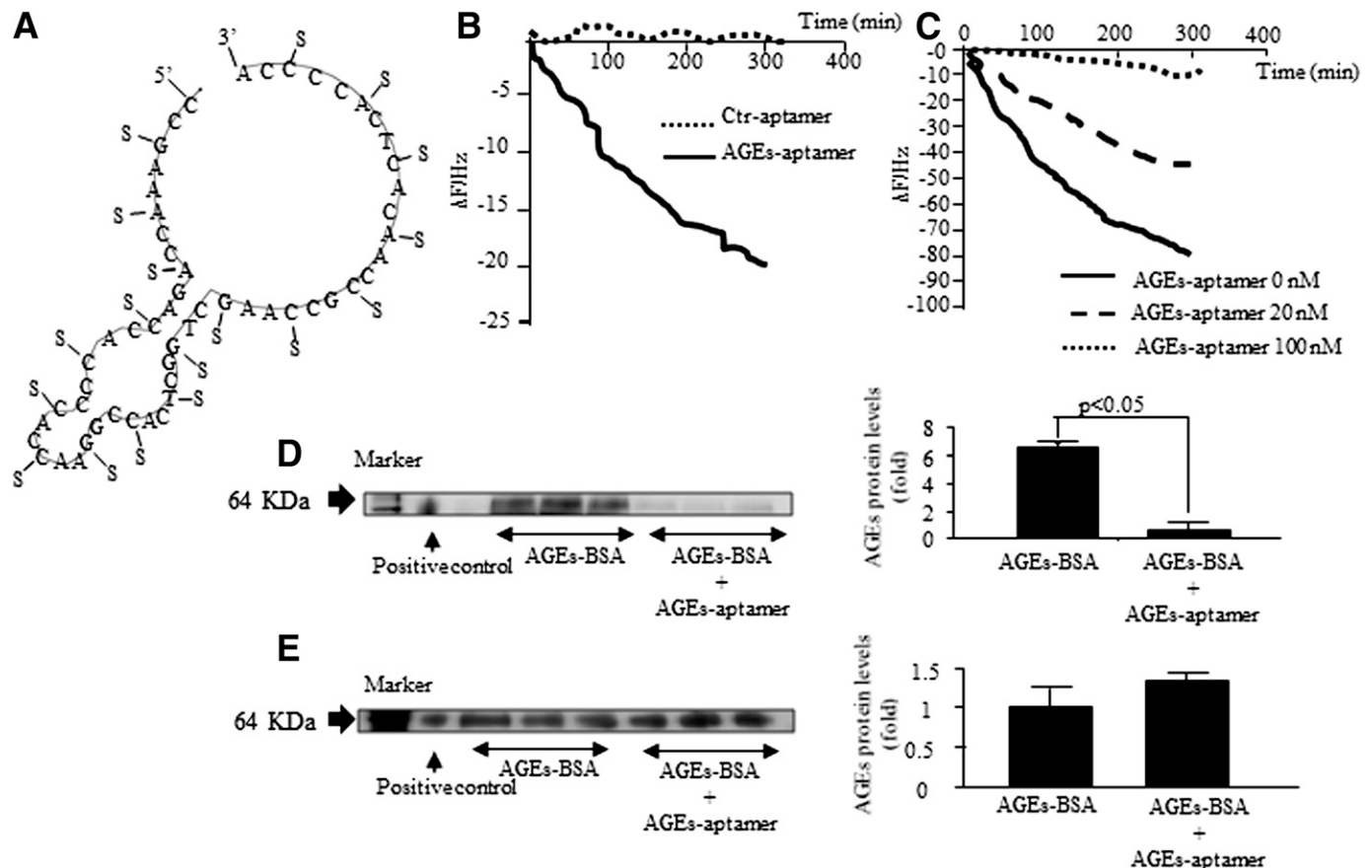
FIG. 1. A: Predicted secondary structure of AGEs-DNA aptamer. AGEs-aptamer was modified with phosphorothioate. A, adenine; C, cytosine; G, guanine; S, phosphorothioate; T, thymine. B: Binding affinity of Ctr- or AGEs-aptamer to AGEs-HSA. n = 4. C: Binding affinity of AGEs-HSA to vRAGE. n = 3. D and E: 100 µg/mL AGEs-BSA was added to the culture medium in the presence or absence of 2 µmol/L AGEs-aptamer where differentiated THP-1 macrophages were grown (D) or ungrown (E). After 4 h, AGE levels in the supernatant were determined with Western blots.
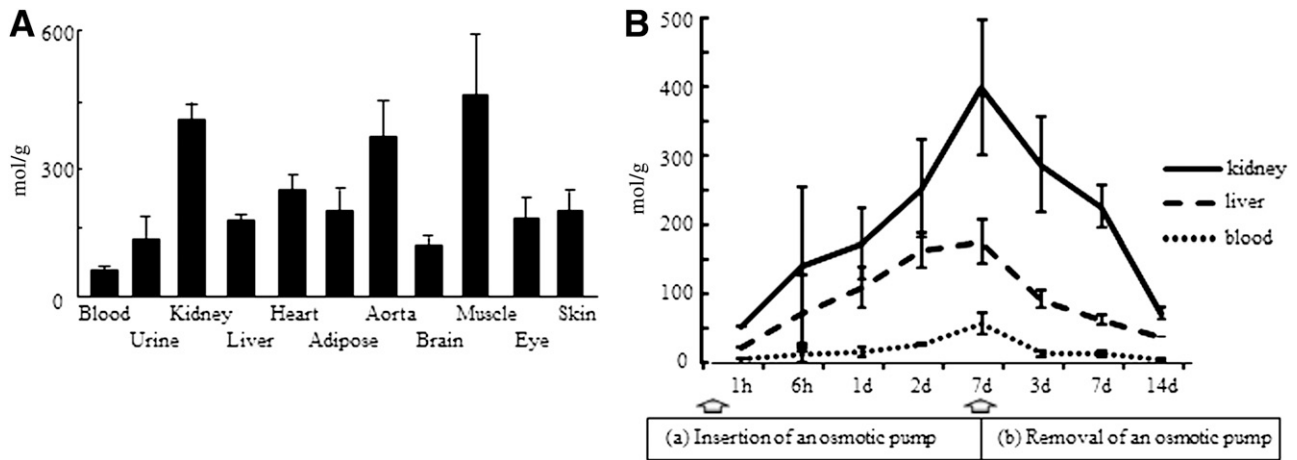
FIG. 2. *A*: Biodistribution of [γ-^{32}P]ATP-labeled AGEs-DNA aptamer. C57BL/6J mice received continuous intraperitoneal infusion of [γ-^{32}P]ATP-labeled AGEs-aptamer for 7 days. Then, blood, urine, and several organs were obtained. [γ-^{32}P]ATP-labeled AGEs-aptamer was detected by Cherenkov counting. Results were presented as mole per gram of tissue. *n* = 3. *B*: Time course kinetics of [γ-^{32}P]ATP-labeled AGEs-aptamer (0.136 μg/day). C57BL/6J mice received continuous intraperitoneal infusion of [γ-^{32}P]ATP-labeled AGEs-aptamer for 7 days. Then, blood, liver, and kidney were obtained. Results are presented as mole per gram of tissue. *n* = 2. d, day.

AGEs in KKAy/Ta mice. As shown in Fig. 3*A*, compared with those in Ctr-Ctr-aptamer mice, serum levels of AGEs were significantly increased to approximately threefold in DM-Ctr-aptamer mice ($P < 0.05$), which were not affected by the treatment with AGEs-aptamer. However, immunohistochemical analysis revealed that AGE levels in the glomeruli of DM-Ctr-aptamer mice were significantly higher than those of Ctr-Ctr-aptamer mice, which was prevented by the treatment with AGEs-aptamer (Fig. 3*B*–*F*). AGEs-aptamer itself did not affect serum or renal levels of AGEs in Ctr mice.

Treatment with AGEs-aptamer decreased UAE levels in DM mice. We examined the effect of AGEs-aptamer on UAE levels in mice. As shown in Fig. 4, UAE levels were gradually and significantly elevated in DM-Ctr-aptamer mice compared with Ctr-Ctr-aptamer mice ($P < 0.01$). Administration of AGEs-aptamer for 8 weeks significantly decreased UAE levels in DM mice ($P < 0.01$). AGEs-aptamer itself did not affect UAE levels in Ctr mice.

Treatment with AGEs-aptamer prevented glomerular hypertrophy and ECM protein accumulation in the kidney of DM mice. Glomerular hypertrophy and ECM accumulation are characteristic features of diabetic nephropathy (3). So, we investigated whether AGEs-aptamer

treatment could prevent the structural changes in the kidney of DM mice. As shown in (Fig. 5*A*–*E*), periodic acid Schiff staining revealed that diabetes was associated with glomerular hypertrophy, which was significantly ameliorated by the administration of AGEs-aptamer. Further, ECM accumulation assessed by Masson trichrom staining was significantly increased in DM-Ctr-aptamer mice, which was also prevented by the treatment with AGEs-aptamer (Fig. 5*F*–*J*). AGEs-aptamer itself did not affect glomerular hypertrophy or ECM accumulation in Ctr mice. Further, immunohistochemical analysis revealed that synaptopodin levels, a marker of podocytes, were reduced in DM-Ctl-aptamer mice, which were significantly restored by the treatment with AGEs-aptamer (Fig. 5*K*–*O*). There was no significant difference of renal VEGF expression, tubulointerstitial fibrosis (data not shown), or *N*-acetyl-β-D-glucosaminidase levels (Table 1) among the groups.

Treatment with AGEs-aptamer decreased urinary excretion levels of 8-OHdG in DM mice. We next examined whether AGEs-aptamer treatment could decrease urinary excretion levels of 8-OHdG, a marker of oxidative stress, in DM mice. Compared with those in Ctr-Ctr-aptamer mice, urinary 8-OHdG levels were significantly increased in DM-Ctr-aptamer mice to ~2.5-fold ($P < 0.05$). Administration

TABLE 1
Characteristics of animals

	Ctr-Ctr-aptamer	Ctr-AGEs-aptamer	DM-Ctr-aptamer	DM-AGEs-aptamer
n	8	9	11	10
Body weight (g)	24.9 ± 1.5	25.1 ± 1.1	45.5 ± 1.2*	43.2 ± 1.2*
Systolic blood pressure (mmHg)	99.7 ± 3.9	107.0 ± 2.7	104.5 ± 2.5	102.6 ± 2.5
Plasma glucose (mg/dL)	177.0 ± 9.9	185.4 ± 9.8	297.9 ± 42.4*	328.2 ± 53.3*
HbA$_{1c}$ (%)	4.0 ± 0.05	4.0 ± 0.08	6.0 ± 0.4*	6.3 ± 0.3*
Total cholesterol (mg/dL)	70.6 ± 2.8	66.1 ± 3.9	103.5 ± 13.9*	88.4 ± 5.3*
Blood urea nitrogen (mg/dL)	34.3 ± 2.1	31.4 ± 2.4	33.3 ± 1.6	28.0 ± 1.2#
Creatinine (mg/dL)	0.14 ± 0.01	0.12 ± 0.01	0.15 ± 0.01	0.10 ± 0.02#
Aspartate aminotransferase (IU/L)	158.4 ± 60.6	149.8 ± 39.9	273.0 ± 105.7	99.5 ± 15.4
Alanine aminotransferase (IU/L)	6.8 ± 3.0	6.5 ± 1.6	29.4 ± 8.0	24.5 ± 11.9
Kidney-to-body weight ratio	13.6 ± 0.7	13.7 ± 0.4	20.3 ± 2.5*	14.8 ± 0.7#
Urinary *N*-acetyl-β-D-glucosaminidase (units/day)	0.22 ± 0.06	0.10 ± 0.01	0.34 ± 0.06	0.26 ± 0.02

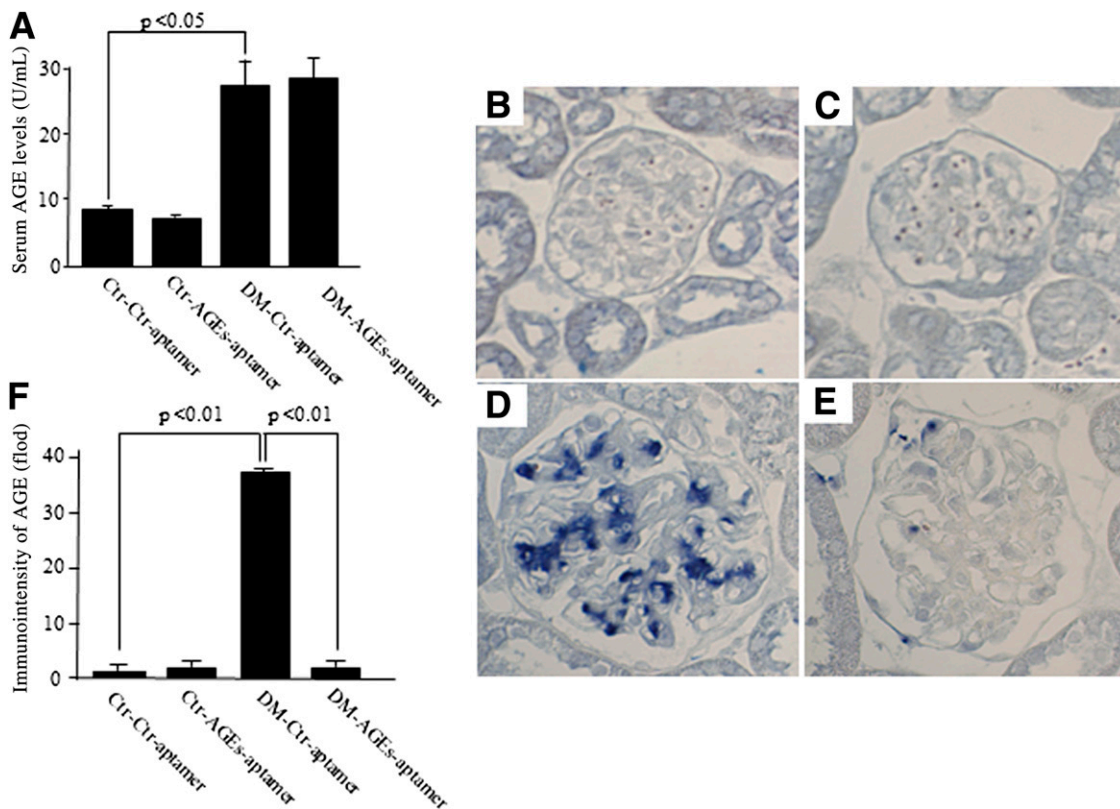Data are means ± SEM. *$P < 0.05$ vs. Ctr-Ctr-aptamer. #$P < 0.05$ vs. DM-Ctr-aptamer.

FIG. 3. Serum and renal levels of AGEs in each animal. *A*: Serum levels of AGEs were measured with ELISA. *n* = 4–5 per group. Representative photographs of AGEs immunostaining in the kidney. Ctr-Ctr-aptamer mice (*B*), Ctr-AGEs-aptamer mice (*C*), DM-Ctr-aptamer mice (*D*), DM-AGEs-aptamer mice (*E*). *F*: Quantitative data of glomerular staining for AGEs. *n* = 4–5 per group. Magnification ×600.

of AGEs-aptamer significantly reduced urinary excretion levels of 8-OHdG in DM mice ($P < 0.05$) (Fig. 5*P*).

Treatment with AGEs-aptamer decreased inflammatory and fibrotic gene expression in the kidney of KKAy/Ta mice. AGEs induce a variety of inflammatory and fibrotic 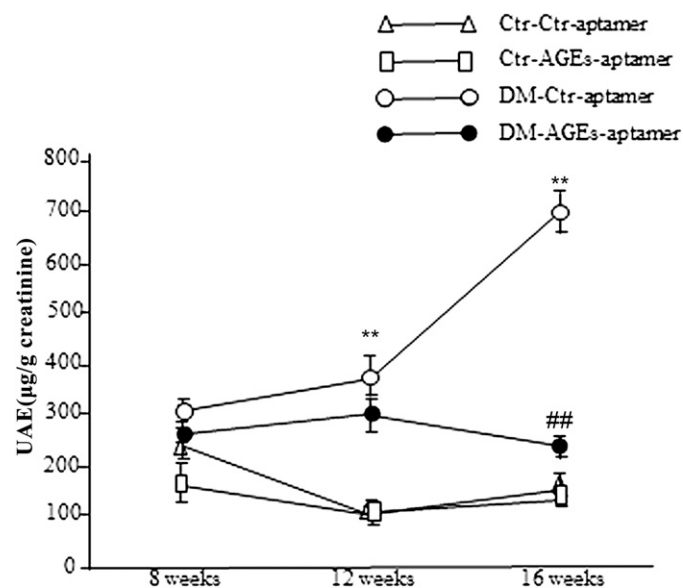gene expression, thus being involved in diabetic nephropathy (16,33,34). So, we studied the effects of AGEs-aptamer on *MCP-1*, *TNF-α*, *CTGF*, type IV collagen, and *RAGE* gene expression in KKAy/Ta mice. As shown in Fig. 6*A–D*, renal *MCP-1*, *TNF-α*, *CTGF*, and type IV collagen gene expression was significantly increased in DM-Ctr-aptamer mice, which was prevented by the administration of AGEs-aptamer. Moreover, although there were no significant differences in gene expression levels of *RAGE* and another AGE-scavenging receptor, *AGE-R3*, between Ctr-Ctr-aptamer and DM-Ctr-aptamer mice, treatment with AGEs-aptamer significantly reduced *RAGE* and *AGE-R3* mRNA levels in the kidney of DM mice (Fig. 6*E* and *F*).

AGEs-aptamer decreased ROS generation and inflammatory and fibrotic gene expression in AGE-exposed human mesangial cells. We next examined whether AGEs-aptamer could inhibit AGE-elicited ROS generation and *RAGE*, *MCP-1*, and *CTGF* gene expression in human mesangial cells. AGEs-BSA (100 μg/mL) for 4 h significantly increased ROS generation (Fig. 7*A*). *RAGE* gene expression was increased at 4 and 24 h after the treatment with AGEs-BSA, whereas *MCP-1* and *CTGF* mRNA levels were elevated at 24 h only (Fig. 7*B–D*). AGEs-aptamer significantly prevented these harmful effects of AGEs, although they did not have any toxic effects on BSA-treated cells. Furthermore, AGEs-BSA for 4 h increased gene expression of *TNF-α* but not *RAGE*, *MCP-1*, or *CTGF* in THP-1 cells, which was also blocked by AGEs-aptamer (data not shown).

DISCUSSION

In the current study, we demonstrate for the first time that although infusion of in vitro–selected DNA-aptamer raised

FIG. 4. Effect of AGEs-aptamer on UAE levels (μg/g creatinine) in each animal. *n* = 8–10 per group. **$P < 0.01$ vs. Ctr-Ctr-aptamer mice. ##$P < 0.01$ vs. DM-Ctr-aptamer mice.
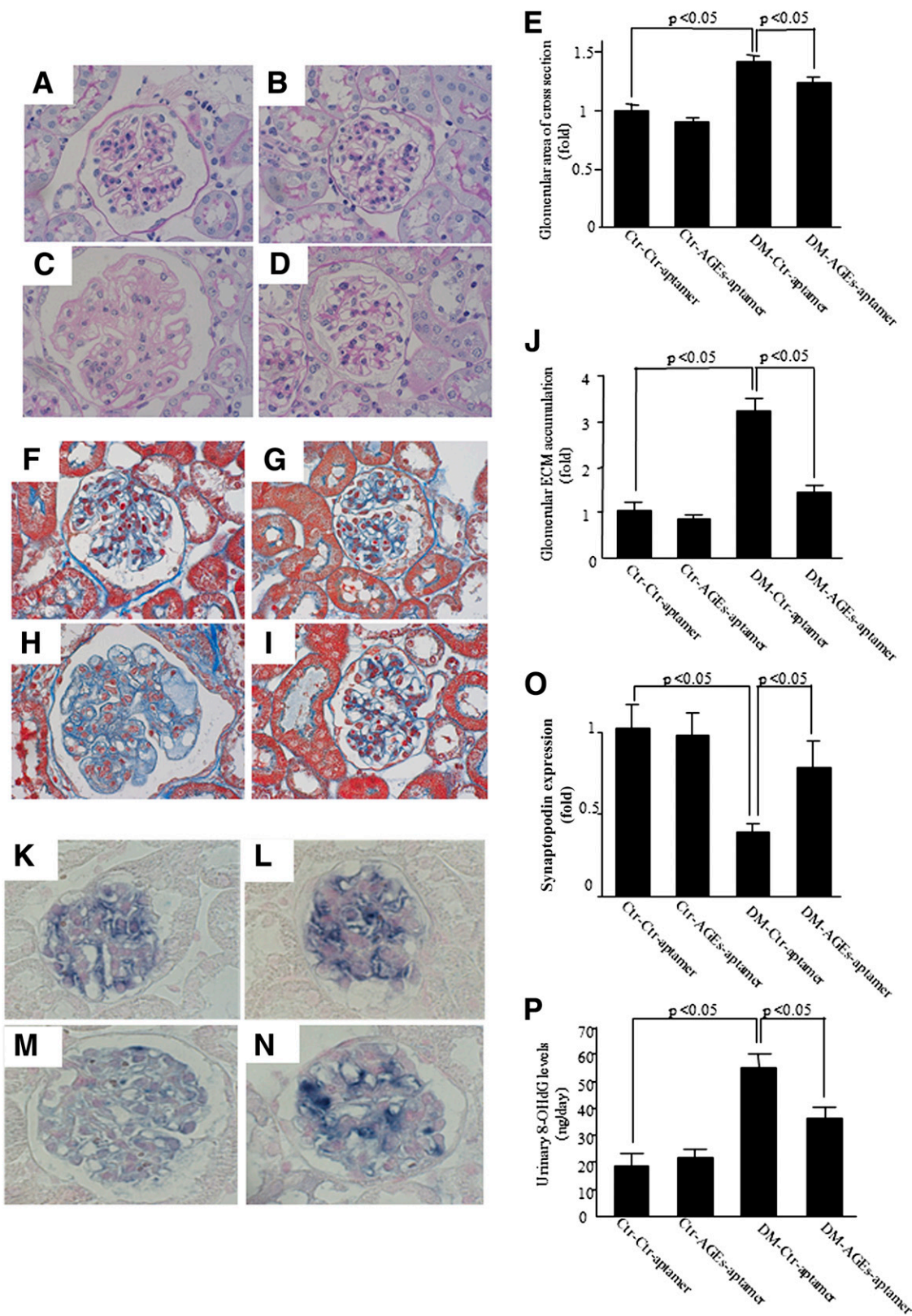
FIG. 5. Representative photographs of glomerular hypertrophy. Glomerular hypertrophy was evaluated by measuring glomerular area of cross-section in the distal cortex. Ctr-Ctr-aptamer mice (*A*), Ctr-AGEs-aptamer mice (*B*), DM-Ctr-aptamer mice (*C*), DM-AGEs-aptamer mice (*D*). *E*: Quantitative data of glomerular area. *n* = 4–5 per group. Magnification ×600. Effect of AGEs-aptamer on glomerular ECM accumulation in each animal. Glomerular ECM accumulation was evaluated by the intensity of Masson trichrome staining in the glomeruli. Representative photographs of the kidney in Ctr-Ctr-aptamer mice (*F*), Ctr-AGEs-aptamer mice (*G*), DM-Ctr-aptamer mice (*H*), and DM-AGEs-aptamer mice (*I*). *J*: Quantitative data of ECM accumulation. *n* = 3–5 per group. Synaptopodin levels in the glomeruli. Representative photographs of the kidney in Ctr-Ctr-aptamer mice (*K*), Ctr-AGEs-aptamer mice (*L*), DM-Ctr-aptamer mice (*M*), and DM-AGEs-aptamer mice (*N*). *O*: Quantitative data of synaptopodin expression. *n* = 3–5 per group. Magnification ×600. *P*: Effect of AGEs-aptamer on urinary 8-OHdG levels (ng/day) in each animal group. Urinary 8-OHdG levels were measured by ELISA. *n* = 8–11 per group.
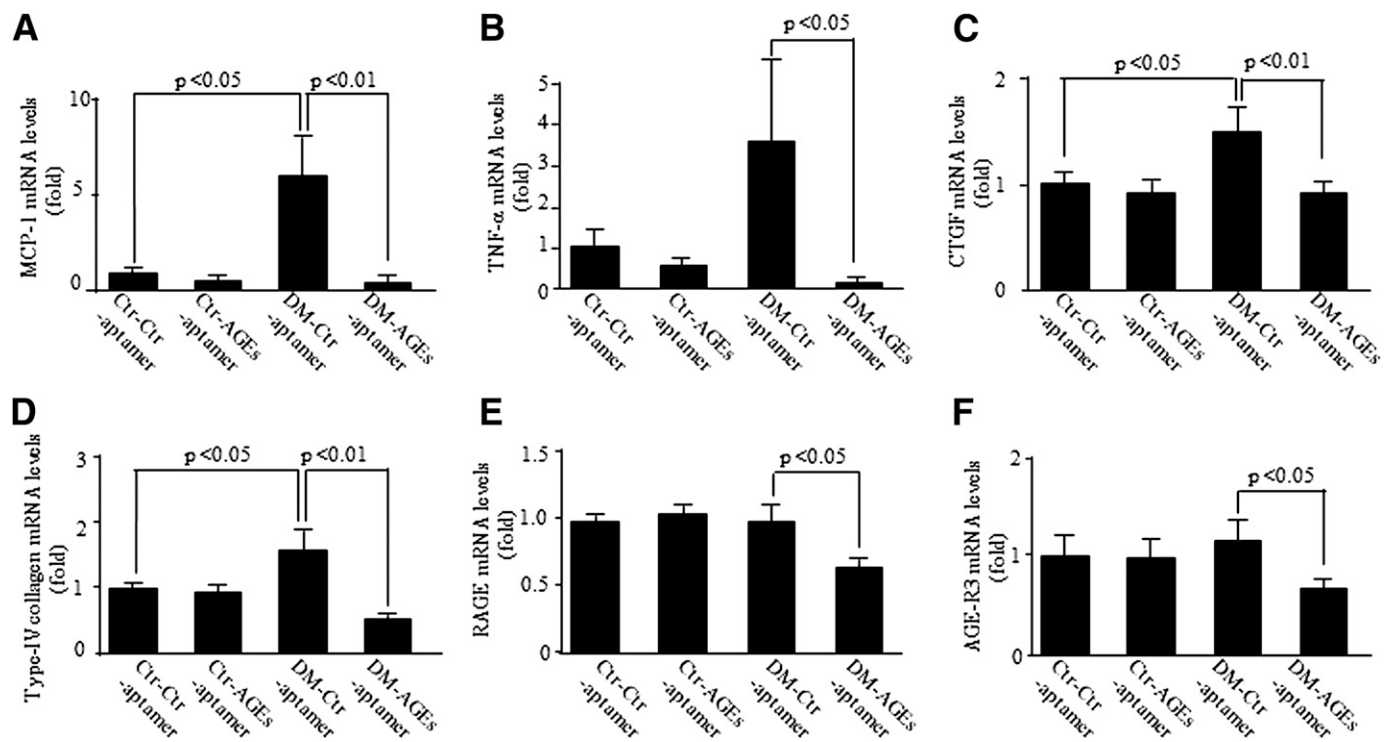
FIG. 6. Effect of AGEs-aptamer on cortical *MCP-1* (*A*), *TNF-α* (*B*), *CTGF* (*C*), type IV collagen (*D*), *RAGE* (*E*), and *AGE-R3* (*F*) gene expression in each animal group. Total RNAs were transcribed and amplified by real-time PCR. Data were normalized by the intensity of 18S rRNA-derived signals and then related to the value obtained with Ctr-Ctr-aptamer mice. $n = 10$–16 per group.

against AGEs-HSA did not affect glucose, HbA_{1c}, or blood pressure levels, it not only inhibited glomerular hypertrophy and ECM protein accumulation but also decreased urinary excretion levels of albumin and 8-OHdG in DM mice. In addition, administration of AGEs-aptamer significantly decreased plasma levels of blood urea nitrogen and creatinine, thus preventing renal dysfunction in DM mice. Moreover, treatment with AGEs-aptamer significantly suppressed *MCP-1*, *TNF-α*, *CTGF*, type IV collagen, and *RAGE* gene expression in the kidney of DM mice, whereas AGEs-aptamer completely blocked the AGE-induced upregulation of *RAGE*, *MCP-1*, and *CTGF* mRNA levels in mesangial cells. In this study, we found that levels of AGEs-aptamer were increased in the kidney of 8-week-old Ctr mice for at least 7 days after the continuous intraperitoneal infusion. Further, at day 14 after stopping the injection, AGEs-aptamer was still detected in the kidney. These findings suggest that phosphorothioate AGEs-aptamer used in these experiments may be resistant to nuclease attack and quite stable and therefore suitable as a therapeutic agent. Given that no toxicities related to AGEs-aptamer were observed after the intraperitoneal injection, our present observations indicate that continuous infusion of AGEs-aptamer may be a safe and effective therapeutic strategy for preventing the development and progression of diabetic nephropathy. However, this will have to be affirmed before widespread clinical use of the AGEs-aptamer is entertained. To compare the efficacy of AGEs-aptamer with other means of reducing the load of AGEs would also be interesting because the latter is mostly delivered orally.

Aptamers have the following advantages over antibodies for blocking the function of targeted proteins: *1*) production of aptamers does not rely on biological systems and can easily be selected and constructed from the oligonucleotide library with low cost and time savings in vitro, *2*) aptamers are quite thermally stable and can be denatured and renatured multiple times without loss of activity and specificity, *3*) aptamers do not have immunogenicity over antibodies, and *4*) small size allows more efficient entry into biological compartments (35,36). There is accumulating evidence that AGEs play a role in various disorders such as Alzheimer disease, cancers, and cardiovascular disease (37–39). Increased formation and accumulation of AGEs could link the increased risks for these disorders to diabetes (37–39). Since feasibility and efficacy of insulin pump therapy have already been established in diabetic patients (40) and because various clinical trials with AGEs inhibitors have been terminated because of the safety concern (41), continuous pump infusion of insulin plus AGEs-aptamer may be promising for preventing various life-threatening AGE-related disorders in diabetes.

In the current study, we demonstrated that continuous infusion of AGEs-aptamer for 8 weeks dramatically decreased AGE levels in the glomeruli of DM mice to basal levels. Engagement of RAGE with AGEs stimulates ROS generation in a variety of cells, which could in turn promote the formation and accumulation of AGEs, thus forming a positive feedback loop between RAGE downstream signaling and AGE generation (16,42). Indeed, aortic AGE accumulation has been suppressed in RAGE-deficient diabetic apolipoprotein E knockout mice (42). In the current study, AGEs-aptamer directly bound to AGEs and resultantly blocked the binding of AGEs to RAGE (Fig. 1*B* and *C*). These observations suggest that AGEs-aptamer could decrease the glomerular accumulation of AGEs via the blockade of AGEs binding to RAGE in the kidney.
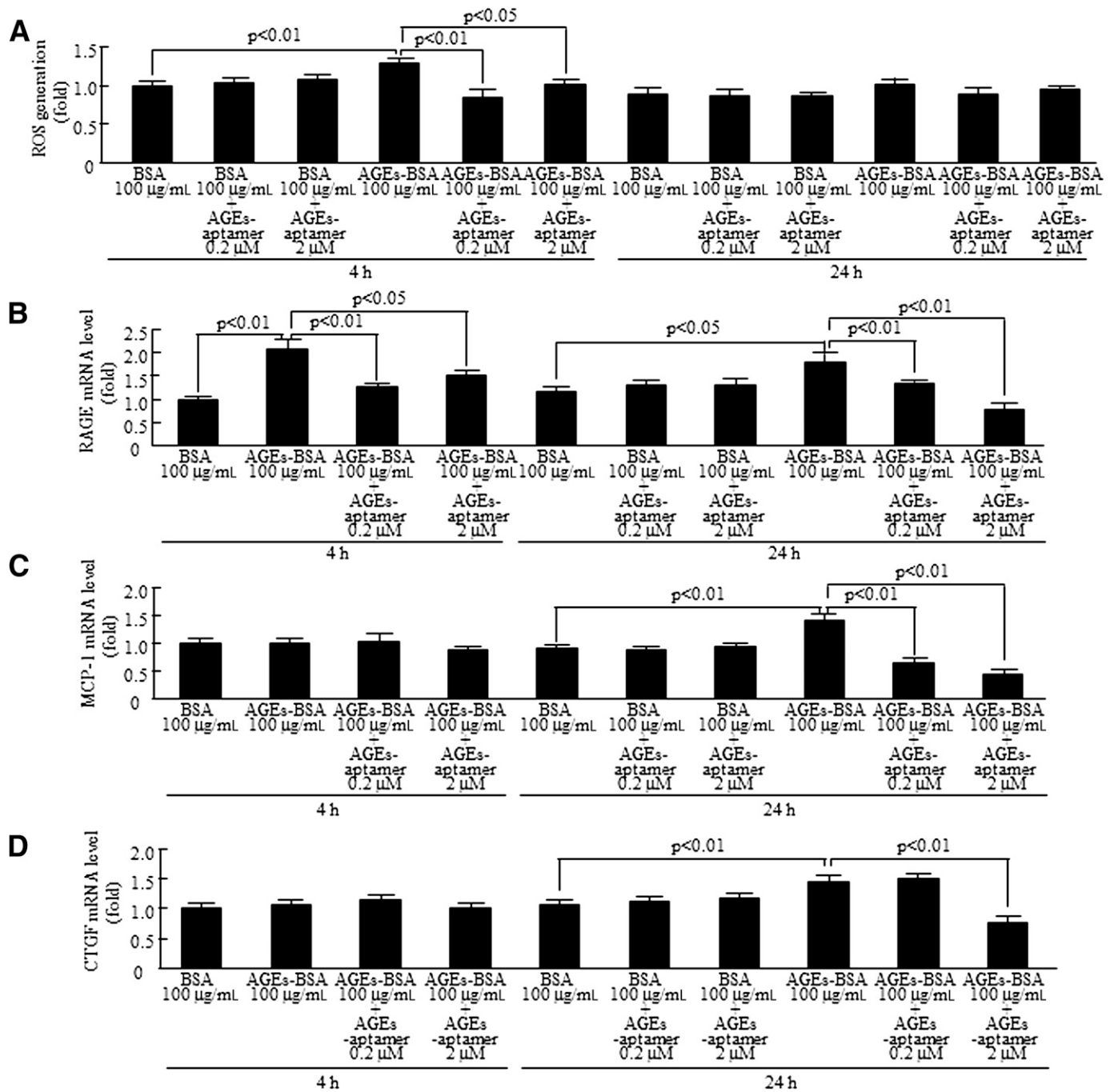
FIG. 7. Effect of AGEs-aptamer on ROS generation (*A*) and *RAGE* (*B*), *MCP-1* (*C*), and *CTGF* (*D*) gene expression in human mesangial cells. Mesangial cells were treated with 100 μg/mL AGEs-BSA or nonglycated BSA for 4 and 24 h in the presence or absence of 0.2 or 2 μmol/L AGEs-aptamer. Total RNAs were transcribed and amplified by real-time PCR. Data were normalized by the intensity of GAPDH mRNA-derived signals and then related to the value obtained with nonglycated BSA. *n* = 3 per group. h, hour.

Further, we found here that turnover rate of aptamer-bound AGEs by THP-1 macrophages was increased compared with that of unbound AGEs (Fig. 1*D*). This is another possible mechanism by which AGEs-aptamer decreased the glomerular accumulation of AGEs. Since treatment with AGEs-aptamer did not affect serum AGE levels in DM mice, AGEs-aptamer may be preferentially distributed and accumulated in the kidney and vessels, locally suppress the actions of AGEs, and finally be eliminated from the body via the increased turnover by macrophages. Under nondiabetic normal conditions, oxidative stress, RAGE

expression, and AGEs accumulation are largely suppressed. This is a possible reason why AGEs-aptamer did not reduce renal AGEs levels of Ctr mice.

AGEs-RAGE interaction elicits inflammatory and fibrotic reactions in the kidney cells via oxidative stress generation (13). In this study, we found that treatment with AGEs-aptamer decreased urinary 8-OHdG and albumin levels and reduced inflammatory and fibrotic gene expression (*MCP-1*, *TNF-α*, *CTGF*, and type IV collagen) in the kidney of DM mice. MCP-1 is a specific chemokine that recruits and activates monocytes from circulation to inflammatory sites

(43). Increased MCP-1 expression associated with monocyte infiltration in mesangial areas has been observed in an early phase of diabetic nephropathy (44). Plasma MCP-1 level was found to be positively correlated with UAE in type 1 diabetic patients (44). Further, administration of AGEs has been shown to cause glomerular hypertrophy and ECM accumulation in the rat kidney via induction of CTGF and type IV collagen expression (45). Since AGEs-aptamer completely blocked the AGE-induced upregulation of *RAGE*, *MCP-1*, and *CTGF* mRNA levels in human mesangial cells, the present findings suggest that blockade of the AGEs-RAGE axis by AGEs-aptamer could decrease albuminuria and fibrotic reactions in the diabetic kidney via suppression of ROS. It would be interesting to examine the effects of AGEs-aptamer on nitrotyrosine levels, another marker of oxidative stress in the diabetic kidney. Further, although decreased synaptopodin levels were restored by AGEs-aptamer, to examine the effects of aptamer on podocyte apoptosis and injury using a cell culture system may be more helpful.

If we assume that volume of distribution for the aptamer is extracellular fluid and that total body water is ~60% of body weight, the concentration of aptamer in mice is estimated to be 1.59×10^{-9} mol/L. Therefore, the estimated delivered dose of aptamer seems to be 880 times less than the measured KD of AGEs-aptamer (1.38×10^{-6} mol/L) at a glance. We may not be able to reconcile the large discrepancy in the delivered dose of AGEs-aptamer and the KD. However, in this study AGEs-aptamer was more accumulated in the kidney compared with the circulating blood; after a 7-day continuous injection, levels of AGEs-aptamer in the kidney were approximately eightfold higher than those in the blood (Fig. 2*A* and *B*). Furthermore, AGEs-aptamer was continuously administered for 8 weeks. So, although the cumulative effect of dosing may plateau or increase in a nonlinear fashion after several weeks of dosing and we did not measure the kidney concentration of the AGEs-aptamer after 8 weeks of treatment, it could be estimated that there is a 64-fold (8×8) preferential distribution of AGEs-aptamer in the glomeruli compared with the blood. In addition, AGEs-aptamer dramatically suppressed the glomerular accumulation of AGEs; the levels in the kidney were decreased to approximately one-twentieth those of Ctr-aptamer–treated DM mice (Fig. 3*F*). These findings suggest that the delivered dose of AGEs-aptamer used here (0.136 µg/day) may not necessarily be insufficient for suppressing the actions of AGEs. We have found in the preliminary animal experiments that intravenous administration of ~70 times higher dose of AGEs-aptamer every other day up to 2 months causes severe diarrhea. This is a rationale for why we chose the original relatively lower dose of AGEs-aptamer in the present experiments.

In the current study, AGEs-aptamer not only inhibited the inflammatory and fibrotic gene expression in both kidney and mesangial cells but also prevented the development of histologic and physiologic parameters associated with experimental diabetic nephropathy. Further, Ctr-aptamer alone did not have any specific actions in either the kidney or mesangial cells. These observations suggest the biological relevance of changes in gene expression, although the differences among the groups are modest. In this study, there were no significant differences in gene expression levels of *RAGE* and *AGE-R3* between Ctr-Ctr-aptamer and DM-Ctr-aptamer mice. However, we performed RT-PCR analysis for *RAGE* and *AGE-R3* genes using whole kidney. So, the gene expression in response to AGEs may be differently regulated in mesangial cells and whole kidney because the latter is mainly composed of tubular cells. Moreover, it would be helpful to determine whether a long-term administration of AGEs-aptamer could stabilize the excretion of albuminuria and resultantly prevent the progression of diabetic nephropathy.

REFERENCES

1. Krolewski AS, Warram JH, Valsania P, Martin BC, Laffel LM, Christlieb AR. Evolving natural history of coronary artery disease in diabetes mellitus. Am J Med 1991;90:56S–61S
2. Maisonneuve P, Agodoa L, Gellert R, et al. Distribution of primary renal diseases leading to end-stage renal failure in the United States, Europe, and Australia/New Zealand: results from an international comparative study. Am J Kidney Dis 2000;35:157–165
3. Mauer SM, Lane P, Hattori M, Fioretto P, Steffes MW. Renal structure and function in insulin-dependent diabetes mellitus and type I membranoproliferative glomerulonephritis in humans. J Am Soc Nephrol 1992;2 (Suppl.):S181–S184
4. Sharma K, Ziyadeh FN. Hyperglycemia and diabetic kidney disease. The case for transforming growth factor-beta as a key mediator. Diabetes 1995; 44:1139–1146
5. Skyler JS, Bergenstal R, Bonow RO, et al.; American Diabetes Association; American College of Cardiology Foundation; American Heart Association. Intensive glycemic control and the prevention of cardiovascular events: implications of the ACCORD, ADVANCE, and VA Diabetes Trials: a position statement of the American Diabetes Association and a Scientific Statement of the American College of Cardiology Foundation and the American Heart Association. J Am Coll Cardiol 2009;53:298–304
6. Brownlee M, Cerami A, Vlassara H. Advanced glycosylation end products in tissue and the biochemical basis of diabetic complications. N Engl J Med 1988;318:1315–1321

7. Grandhee SK, Monnier VM. Mechanism of formation of the Maillard protein cross-link pentosidine. Glucose, fructose, and ascorbate as pentosidine precursors. J Biol Chem 1991;266:11649–11653

8. Dyer DG, Blackledge JA, Thorpe SR, Baynes JW. Formation of pentosidine during nonenzymatic browning of proteins by glucose. Identification of glucose and other carbohydrates as possible precursors of pentosidine in vivo. J Biol Chem 1991;266:11654–11660

9. Genuth S, Sun W, Cleary P, et al.; DCCT Skin Collagen Ancillary Study Group. Glycation and carboxymethyllysine levels in skin collagen predict the risk of future 10-year progression of diabetic retinopathy and nephropathy in the diabetes control and complications trial and epidemiology of diabetes interventions and complications participants with type 1 diabetes. Diabetes 2005;54:3103–3111

10. Thomas MC, Forbes JM, Cooper ME. Advanced glycation end products and diabetic nephropathy. Am J Ther 2005;12:562–572

11. Nożyński J, Zakliczyński M, Konecka-Mrowka D, et al. Advanced glycation end product accumulation in the cardiomyocytes of heart failure patients with and without diabetes. Ann Transplant 2012;17:53–61

12. Beisswenger PJ, Drummond KS, Nelson RG, Howell SK, Szwergold BS, Mauer M. Susceptibility to diabetic nephropathy is related to dicarbonyl and oxidative stress. Diabetes 2005;54:3274–3281

13. Fukami K, Yamagishi S, Ueda S, Okuda S. Role of AGEs in diabetic nephropathy. Curr Pharm Des 2008;14:946–952

14. Coughlan MT, Thorburn DR, Penfold SA, et al. RAGE-induced cytosolic ROS promote mitochondrial superoxide generation in diabetes. J Am Soc Nephrol 2009;20:742–752

15. Tsuchida K, Makita Z, Yamagishi S, et al. Suppression of transforming growth factor beta and vascular endothelial growth factor in diabetic nephropathy in rats by a novel advanced glycation end product inhibitor, OPB-9195. Diabetologia 1999;42:579–588

16. Yamagishi S, Imaizumi T. Diabetic vascular complications: pathophysiology, biochemical basis and potential therapeutic strategy. Curr Pharm Des 2005;11:2279–2299

17. Yamamoto Y, Kato I, Doi T, et al. Development and prevention of advanced diabetic nephropathy in RAGE-overexpressing mice. J Clin Invest 2001; 108:261–268

18. Bock LC, Griffin LC, Latham JA, Vermaas EH, Toole JJ. Selection of single-stranded DNA molecules that bind and inhibit human thrombin. Nature 1992;355:564–566

19. Gragoudas ES, Adamis AP, Cunningham ET Jr, Feinsod M, Guyer DR; VEGF Inhibition Study in Ocular Neovascularization Clinical Trial Group. Pegaptanib for neovascular age-related macular degeneration. N Engl J Med 2004;351:2805–2816

20. Jilma-Stohlawetz P, Gilbert JC, Gorczyca ME, Knöbl P, Jilma B. A dose ranging phase I/II trial of the von Willebrand factor inhibiting aptamer ARC1779 in patients with congenital thrombotic thrombocytopenic purpura. Thromb Haemost 2011;106:539–547

21. Markus HS, McCollum C, Imray C, Goulder MA, Gilbert J, King A. The von Willebrand inhibitor ARC1779 reduces cerebral embolization after carotid endarterectomy: a randomized trial. Stroke 2011;42:2149–2153

22. Hagiwara S, Makita Y, Gu L, et al. Eicosapentaenoic acid ameliorates diabetic nephropathy of type 2 diabetic KKAy/Ta mice: involvement of MCP-1 suppression and decreased ERK1/2 and p38 phosphorylation. Nephrol Dial Transplant 2006;21:605–615

23. Takeuchi M, Makita Z, Bucala R, Suzuki T, Koike T, Kameda Y. Immunological evidence that non-carboxymethyllysine advanced glycation end-products are produced from short chain sugars and dicarbonyl compounds in vivo. Mol Med 2000;6:114–125

24. Higashimoto Y, Yamagishi S, Nakamura K, et al. In vitro selection of DNA aptamers that block toxic effects of AGE on cultured retinal pericytes. Microvasc Res 2007;74:65–69

25. King DJ, Ventura DA, Brasier AR, Gorenstein DG. Novel combinatorial selection of phosphorothioate oligonucleotide aptamers. Biochemistry 1998;37:16489–16493

26. Okahata Y, Niikura K, Sugiura Y, Sawada M, Morii T. Kinetic studies of sequence-specific binding of GCN4-bZIP peptides to DNA strands immobilized on a 27-MHz quartz-crystal microbalance. Biochemistry 1998;37: 5666–5672

27. Yamagishi S, Inagaki Y, Amano S, Okamoto T, Takeuchi M, Makita Z. Pigment epithelium-derived factor protects cultured retinal pericytes from advanced glycation end product-induced injury through its antioxidative properties. Biochem Biophys Res Commun 2002;296:877–882

28. Suga T, Iso T, Shimizu T, et al. Activation of receptor for advanced glycation end products induces osteogenic differentiation of vascular smooth muscle cells. J Atheroscler Thromb 2011;18:670–683

29. Inagaki Y, Yamagishi S, Amano S, Okamoto T, Koga K, Makita Z. Interferon-gamma-induced apoptosis and activation of THP-1 macrophages. Life Sci 2002;71:2499–2508

30. Ojima A, Ishibashi Y, Matsui T, et al. Glucagon-like peptide-1 receptor agonist inhibits asymmetric dimethylarginine generation in the kidney of streptozotocin-induced diabetic rats by blocking advanced glycation end product-induced protein arginine methyltranferase-1 expression. Am J Pathol 2013;182:132–141

31. Takamiya Y, Fukami K, Yamagishi SI, et al. Experimental diabetic nephropathy is accelerated in matrix metalloproteinase-2 knockout mice. Nephrol Dial Transplant 2013;28:55–62

32. Matsui T, Nishino Y, Takeuchi M, Yamagishi S. Vildagliptin blocks vascular injury in thoracic aorta of diabetic rats by suppressing advanced glycation end product-receptor axis. Pharmacol Res 2011;63:383–388

33. Fukami K, Ueda S, Yamagishi S, et al. AGEs activate mesangial TGF-beta-Smad signaling via an angiotensin II type I receptor interaction. Kidney Int 2004;66:2137–2147

34. Matsui T, Yamagishi S, Takeuchi M, Ueda S, Fukami K, Okuda S. Irbesartan inhibits advanced glycation end product (AGE)-induced proximal tubular cell injury in vitro by suppressing receptor for AGEs (RAGE) expression. Pharmacol Res 2010;61:34–39

35. Osborne SE, Matsumura I, Ellington AD. Aptamers as therapeutic and diagnostic reagents: problems and prospects. Curr Opin Chem Biol 1997; 1:5–9

36. Famulok M, Hartig JS, Mayer G. Functional aptamers and aptazymes in biotechnology, diagnostics, and therapy. Chem Rev 2007;107:3715–3743

37. Takeuchi M, Kikuchi S, Sasaki N, et al. Involvement of advanced glycation end-products (AGEs) in Alzheimer's disease. Curr Alzheimer Res 2004;1:39–46

38. Abe R, Yamagishi S. AGE-RAGE system and carcinogenesis. Curr Pharm Des 2008;14:940–945

39. Yamagishi S, Nakamura K, Matsui T, Ueda S, Noda Y, Imaizumi T. Inhibitors of advanced glycation end products (AGEs): potential utility for the treatment of cardiovascular disease. Cardiovasc Ther 2008;26:50–58

40. Bergenstal RM, Tamborlane WV, Ahmann A, et al.; STAR 3 Study Group. Effectiveness of sensor-augmented insulin-pump therapy in type 1 diabetes. N Engl J Med 2010;363:311–320

41. Fukami K, Yamagishi S, Ueda S, Okuda S. Novel therapeutic targets for diabetic nephropathy. Endocr Metab Immune Disord Drug Targets 2007;7: 83–92

42. Soro-Paavonen A, Watson AM, Li J, et al. Receptor for advanced glycation end products (RAGE) deficiency attenuates the development of atherosclerosis in diabetes. Diabetes 2008;57:2461–2469

43. Wenzel UO, Abboud HE. Chemokines and renal disease. Am J Kidney Dis 1995;26:982–994

44. Banba N, Nakamura T, Matsumura M, Kuroda H, Hattori Y, Kasai K. Possible relationship of monocyte chemoattractant protein-1 with diabetic nephropathy. Kidney Int 2000;58:684–690

45. Zhou G, Li C, Cai L. Advanced glycation end-products induce connective tissue growth factor-mediated renal fibrosis predominantly through transforming growth factor beta-independent pathway. Am J Pathol 2004; 165:2033–2043